A static and free vibration analysis method for non-prismatic composite beams with a non-uniform flexible shear connection

Nijgh, Martin; Veljkovic, Milan

DOI
10.1016/j.ijmecsci.2019.06.018

Publication date
2019

Document Version
Final published version

Published in
International Journal of Mechanical Sciences

International Journal of Mechanical Sciences 159 (2019) 398–405

Contents lists available at ScienceDirect

International Journal of Mechanical Sciences

journal homepage: www.elsevier.com/locate/ijmecsci

A static and free vibration analysis method for non-prismatic composite beams with a non-uniform flexible shear connection

Martin Paul Nijgh*, Milan Veljkovic

Faculty of Civil Engineering and Geosciences, Delft University of Technology, Stevinweg 1, 2628 CN, Delft, The Netherlands

ARTICLE INFO

Keywords:
Composite beam
Analytical modelling
Eigenfrequency
Tapered beam
Sustainability

ABSTRACT

Steel-concrete composite beams are widely used in practice because of their economic cross-section design. As sustainability becomes more and more important in the construction industry, the design of composite beams must be adapted to meet the requirements of the circular economy. This calls for demountability and reusability of the structural components, as well as optimized use of materials, for example by using non-prismatic beams. Linear-elastic design and the (optimized) use of demountable shear connectors are key in the design of reusable composite structures. In this paper, analytical prediction models for the elastic behaviour and the first eigenfrequency of non-prismatic composite beams with non-uniform shear connector arrangements are derived. The approach is based on 6th and 2nd order differential equations used to define matrix equations for a finite number of linearized composite beam segments. The analytical models are validated using experimental and numerical results obtained with a simply supported tapered composite beam. The analytical models are suitable for comprehensive structural analysis of non-prismatic composite beams with non-uniform shear connection.

1. Introduction

Composite action between a steel beam and a concrete deck is traditionally achieved using welded headed studs. The mechanical behaviour of welded headed studs is well established in literature (e.g. [1–4]) and therefore included in design codes. Although the use of the welded headed stud is widespread, the main drawback of this type of shear connector is that it does not allow for non-destructive separation of the steel beam and concrete deck [5,6]. Once the building has become obsolete, demolition is the only option to take the building apart.

Demountable shear connectors are increasingly gaining interest in the research field of composite structures, as they do allow for non-destructive separation of the steel beam and concrete deck and thereby score comparatively better in sustainability assessment. Demountability of the shear connection offers the possibility to reuse the structure, either by changing the floor plan to allow for different functional use and/or by re-erecting the entire structure at another location. By designing a structure to be suitable for demountability or reusability, its service lifetime is no longer controlled by its functional lifetime on a specific construction site but by its technical lifetime [7].

The main barriers to designing demountable and reusable composite structures have been identified by Tingly & Davison [8] as:

- Perceived risk in specifying reused materials,
- Additional costs related to the measures related to demountability,
- Composite construction,
- Lack of a reused material market,
- Longer deconstruction time.

The potential barriers must be mitigated to allow the implementation of demountable and reusable structures in practice. The feasibility of construction and execution of demountable and reusable composite beams was recently demonstrated by Nijgh et al. [9] by using large prefabricated concrete decks, a tapered steel beam and demountable shear connectors, in combination with oversized holes and resin-injected bolts. In addition, investigations are on-going which address the (de)construction time and additional costs related to demountable and reusable composite structures.

Steel-concrete composite beams are generally prismatic, i.e. their cross-section does not vary along the beam length. However, tapered composite beams offer both structural and functional advantages compared with prismatic composite beams. Recently, Nijgh et al. [9] conducted experiments to determine the elastic mechanical behaviour of tapered composite beams with various arrangements of demountable shear connectors. It was found that the elastic behaviour of simply supported composite beams could be optimised by concentrating the shear connectors near the supports. This finding is in line with the theoretical predictions by Roberts [10] and Lin et al. [11].

The design of composite beams is governed either by serviceability criteria or by its resistance in the ultimate limit state. In both design cases, a composite beam can be designed to be demountable and

* Corresponding author.
E-mail address: M.P.Nijgh@tudelft.nl (M.P. Nijgh).

https://doi.org/10.1016/j.ijmecsci.2019.06.018
Received 31 January 2019; Received in revised form 29 May 2019; Accepted 8 June 2019
Available online 9 June 2019

reusable as long as the elastic limits are not exceeded. In addition, the perception of human comfort must be considered by designing for a sufficiently high first eigenfrequency.

In the comparative study of Ranzi et al. [12], four different modelling methods for composite beams are outlined:

1 Exact analytical methods
2 Finite difference method
3 Finite element method
4 Direct stiffness method

Exact analytical methods are based on solving differential equations obtained by considering the strain diagram and internal equilibrium of composite beams. The elastic mechanical behaviour of composite beams with flexible (non-rigid) shear connectors was first described analytically by Newmark et al. [13]. The Newmark model consists of two Euler-Bernoulli beams (one representing the steel beam, and the other representing the concrete deck) which are coupled at the interface using a uniformly distributed shear connection. Girhammar & Pan [14] and Girhammar [15] studied the elastic behaviour of composite beams using the Newmark approach, whereas Xu & Wu [16] and Schabl et al. [17] also implemented shear deformation in their models by using Timoshenko beam theory. Yam & Chapman [18] extended the original Newmark model to account for nonlinear material and shear connector behaviour. The exact analytical methods are not directly suitable for accounting for non-uniform shear connector arrangements. An attempt to model non-uniform shear connector arrangements using analytical methods was made by Lawson et al. [19] by assuming the slip distribution to be cosinusoidal. However, the shape function of the slip distribution along the beam length might not be readily predefined for non-prismatic composite beams with (highly) non-uniform shear connector arrangements.

Finite difference methods approximate the behaviour of composite beams numerically by assuming derivatives in the form of algebraic expressions. This modelling method has been developed extensively by Adekola [20], Roberts [10], and Roberts & Al-Amery [21].

Finite element methods provide numerical solutions and are robust and reliable in case suitable shape functions are chosen [12] to approximate the displacements. The finite element formulations are based on Euler–Bernoulli beam theory (e.g. [22,23]), Timoshenko beam theory (e.g. [24,25]) or higher order beam theories (e.g. [26,27]).

The direct stiffness method is based on an initially undeformed element that is subjected to a unit rotation or translation in one of the degrees of freedom (DOF), whilst restraining all other DOFs. The direct stiffness method is presented in the work of Ranzi et al. [28], and later extended by Ranzi & Bradford [29] to account for time-dependent effects.

In this work, analytical prediction models for the elastic behaviour and the first eigenfrequency of non-prismatic composite beams with non-uniform shear connector arrangement are derived. The starting point for the prediction models is to discretise the composite beam into segments, which individually fulfil the basic assumptions of the analytical Newmark model. The results of the proposed analytical models for non-prismatic composite beams with non-uniform shear connector arrangements are compared with the results of actual experiments and/or the results of finite element analysis.

2. Theoretical background

The starting point for the analytical models for the elastic mechanical behaviour and eigenfrequency of non-prismatic composite beams is the partial differential equation, Eq. (1) [16], valid for prismatic composite beams with uniformly distributed flexible shear connectors subject to bending deformation. For the derivation of Eq. (1), the reader is referred to the work of Xu & Wu [16]. Other researchers (e.g. Girhammer et al. [30]) have also derived Eq. (1), although with different notations.

$$\frac{\partial^6 w}{\partial x^6} - \alpha^2 \frac{\partial^4 w}{\partial x^4} + \beta^2 \gamma_1 \frac{\partial^4 w}{\partial x^2 \partial t^2} - \alpha^2 \gamma_1 \frac{\partial^2 w}{\partial t^2} = -\frac{\alpha^2}{EI_\infty} q + \frac{1}{EI_0} \frac{\partial^2 q}{\partial x^2}. \tag{1}$$

$$\alpha^2 = \frac{K \cdot r}{EI_0 \left(1 - \frac{EI_0}{EI_\infty}\right)};\ \beta^2 = \frac{EI_\infty}{EI_0};\ \gamma_1 = \frac{m}{EI_\infty}. \tag{2}$$

$$K = \frac{k_{sc}}{s};\ \ m = \rho_s A_s + \rho_{deck} A_{deck} \tag{3}$$

In Eq. (1), w is the deflection function and α^2, β^2 and γ_1 are geometrical and shear connection parameters defined in Eq. (2). The distributed load (force per unit length) acting on the beam is denoted by q. EI_∞ and EI_0 denote the bending stiffness in case of rigid and no shear connection, respectively. The distance between the elastic neutral axes of the connected members under the assumption of no shear interaction is represented by r. The smeared shear connection stiffness is denoted by K, and is defined as the shear connector stiffness k_{sc} divided by the (uniform) connector spacing s. The mass per unit length is denoted by m. The convention of internal and external actions is defined in Fig. 1.

The shear deformation originating from the transversal load is not included in the analysis, because deflection due to bending is dominant for composite beams with typical span over depth ratios. The rotational inertia is also disregarded because its influence on the lower eigenfrequencies is negligible [16].

Eq. (1) is only valid for prismatic beams with uniformly distributed shear connectors. A discretisation of the beam into J segments is performed along the length of the composite beam to account on the non-uniform shear connector arrangements and varying geometry of the composite beam. Such a discretisation process was first adopted by Taleb & Suppiger [31] to model the free vibrations of non-composite beams, but such an approach has not yet been applied to composite beams with a flexible shear connection. The discretisation process creates a stepped beam with different geometrical and mechanical properties in each segment, as illustrated in Fig. 2. The geometrical and mechanical properties of a segment are determined based on the magnitudes of the influencing variables in the segment's centre. In each segment, the shear connection is assumed continuous (smeared) over the segment length. It is assumed that all materials behave elastically and that the curvature of the constituent members is equal in each cross-section. Therefore, each beam segment fulfils the basic assumptions of the Newmark model.

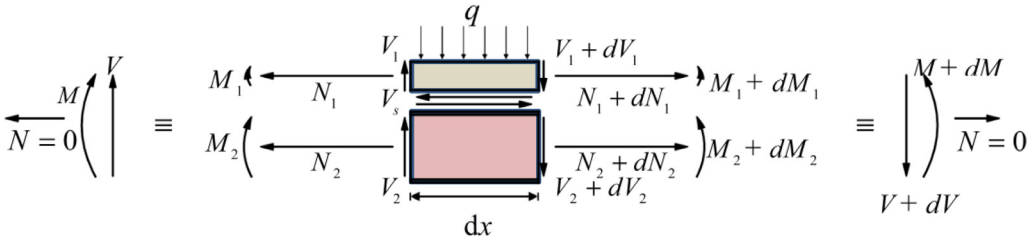

Fig. 1. Convention of internal actions in the differential element of a composite beam with a flexible shear connection. The resultant of the normal force is zero under the assumption that no external axial load is applied.

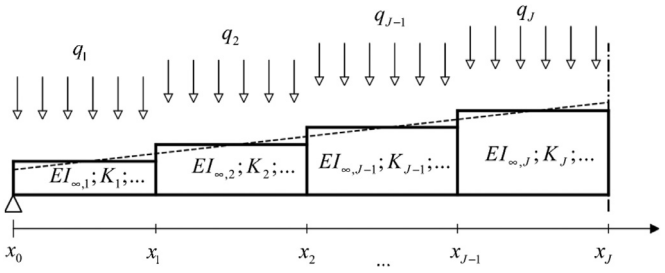

Fig. 2. Discretization of a tapered composite beam (dashed line) into J prismatic composite beam segments of equal length, subject to a uniformly distributed load.

2.1. Static analysis

For composite beams subject to static uniformly distributed loads, Eq. (1) reduces to

$$\frac{d^6w}{dx^6} - \alpha^2\frac{d^4w}{dx^4} = -\frac{\alpha^2}{EI_\infty}q + \frac{1}{EI_0}\frac{d^2q}{dx^2}. \tag{4}$$

Discretising the beam into J segments of equal length (see Fig. 2), and assuming that the applied load per unit length q is constant in each beam segment, Eq. (4) further reduces to

$$\frac{d^6w_j}{dx^6} - \alpha_j^2\frac{d^4w_j}{dx^4} = -\frac{\alpha_j^2}{EI_{\infty,j}}q_j, \tag{5}$$

with $1 \le j \le J$. The solution to this sixth order linear differential equation is given by

$$w_j(x) = C_{1,j}\frac{e^{\alpha_j x}}{\alpha_j^4} + C_{2,i}\frac{e^{-\alpha_j x}}{\alpha_j^4} + C_{3,j}x^3 + C_{4,j}x^2 + C_{5,j}x + C_{6,j} + \frac{1}{24}\frac{q_j x^4}{EI_{\infty,j}}. \tag{6}$$

Expressions for the bending moment$M$, shear force V, shear flow V_s, normal force N_1 and interlayer slip Δu are given by Eqs. (7)–(11), respectively [14,16,30].

$$M_j = \frac{EI_{\infty,j}}{\alpha_j^2}\left[-\frac{d^4w_j}{dx^4} + \alpha_j^2\frac{d^2w_j}{dx^2} + \frac{q_j}{EI_{0,j}}\right] \tag{7}$$

$$V_j = -\frac{dM_j}{dx} = \frac{EI_{\infty,j}}{\alpha_j^2}\left[\frac{d^5w_j}{dx^5} - \alpha_j^2\frac{d^3w_j}{dx^3} - \frac{1}{EI_{0,j}}\frac{dq_j}{dx}\right] \tag{8}$$

$$V_{s,j} = \frac{1}{r_j}\left[V_j + EI_{0,j}\frac{d^3w_j}{dx^3}\right] \tag{9}$$

$$N_{1,j} = \frac{EI_{\infty,j}}{\alpha_j^2 r_j}\left[-\frac{d^4w_j}{dx^4} + \alpha_j^2\left(1 - \frac{EI_{0,j}}{EI_{\infty,j}}\right)\frac{d^2w_j}{dx^2} + \frac{q_j}{EI_{0,j}}\right] \tag{10}$$

$$\Delta u_j = \frac{dN_{1,j}}{dx}\frac{1}{K_j} \tag{11}$$

The 6 J integration constants ($C_{1,1}$, $C_{2,1}$...$C_{5,J}$, $C_{6,J}$), resulting from the J segments in which Eq. (6) is defined, can be solved by imposing boundary conditions at x_0 and x_J, and interface conditions at x_1...x_{J-1}. For a beam simply supported at $x_0 = 0$ and $x_J = L$, the six boundary conditions are $w_1(0) = 0$, $w_J(L) = 0$, $M_1(0) = 0$, $M_J(L) = 0$, $w''''_1\ (0) = q_1/EI_{0,1}$ and $w''''_J\ (L) = q_J/EI_{0,J}$. For a symmetrical simply supported composite beam, the boundary conditions can also be expressed at $x_J = L/2$ as $w'_J(L/2) = 0$, $V_J(L/2) = 0$, and $\Delta u_J(L/2) = 0$.Other types of supporting conditions can be included by modifying the boundary conditions appropriately. The equilibrium of shear force, bending moment and normal force, as well as the continuity of deflection, slope and slip is enforced at the interface of neighbouring segments. These interface conditions are expressed as $w_j(x_j) = w_{j+1}(x_j)$, $w'_j(x_j) = w'_{j+1}(x_j)$, $M_j(x_j) = M_{j+1}(x_j)$, $\Delta u_j(x_j) = \Delta u_{j+1}(x_j)$, $V_j(x_j) = V_{j+1}(x_j)$, and $N_{1,j}(x_j) = N_{1,j+1}(x_j)$. Any concentrated forces can be applied by imposing these in the interface conditions related to the vertical force equilibrium.

2.2. Free vibration analysis

The n-th eigenfrequency of a prismatic beam with a span L, a uniformly distributed mass m and constant bending stiffness EI is given by

$$f_n = \frac{K_n}{2\pi}\sqrt{\frac{EI}{mL^4}}, \tag{12}$$

in which K_n is a constant depending on the boundary conditions. The most important observation from Eq. (12) is that $f_n \sim \sqrt{EI}$. Assuming that the bending stiffness of the beam A with the n-th eigenfrequency $f_{n,A}$ is EI_A, and that the mass per unit length and the span of the beam A and B are equal, the n-th eigenfrequency of the beam B equals

$$f_{n,B} = f_{n,A}\sqrt{\frac{EI_B}{EI_A}}. \tag{13}$$

For tapered composite beams, the bending stiffness is not constant along the beam axis, and therefore the deflection at mid-span under the self-weight can be assumed to be a measure for the beam stiffness instead. The preceding leads to the hypothesis that the natural frequency of a tapered composite beam can be determined using the expression

$$f_n = f_{n,\infty}\sqrt{\frac{w_{m,\infty}}{w_m}}, \tag{14}$$

in which $f_{n,\infty}$ is the n-th natural frequency of the (non-prismatic) composite beam under the assumption of rigid shear connection. w_m and $w_{m,\infty}$ denote the deflection at midspan because of the self-weight imposted along the beam axis in case of flexible and rigid shear connection, respectively. The magnitudes of w_m and $w_{m,\infty}$ for a given beam design can be computed using the analytical method presented in Section 2.1.

The natural frequency $f_{n,\infty}$ of the composite beam with rigid shear connection can be determined using Eq. (15) [31], which is based on Euler-Bernoulli beam theory.

$$EI_\infty\frac{\partial^4w(x,t)}{\partial x^4} = m\frac{\partial^2w(x,t)}{\partial t^2} \tag{15}$$

Eq. (15) can be simplified by using the principle of separation of variables in the form $w(x,t) = \widetilde{w}(x)\exp(i\omega_n t)$. Inserting this expression into Eq. (15) gives

$$\frac{d^4\widetilde{w}}{dx^4} - \zeta^4\widetilde{w} = 0, \tag{16}$$

in which

$$\zeta^4 = \frac{m\omega_{n,\infty}^2}{EI_\infty}. \tag{17}$$

In Eq. (17), $\omega_{n,\infty}$ is a trial solution for the angular eigenfrequency of the full-interaction composite beam. The angular eigenfrequency $\omega_{n,\infty}$ and the eigenfrequency $f_{n,\infty}$ are related to each other by

$$f_{n,\infty} = \frac{\omega_{n,\infty}}{2\pi}. \tag{18}$$

The general solution of Eq. (16) can be expressed in the form

$$\widetilde{w}(x) = C_1\sin(\zeta x) + C_2\cos(\zeta x) + C_3\sinh(\zeta x) + C_4\cosh(\zeta x). \tag{19}$$

The general solution in each of the beam segments is written as

$$\widetilde{w}_j(x) = C_{1,j}\sin(\zeta_j x) + C_{2,j}\cos(\zeta_j x) + C_{3,j}\sinh(\zeta_j x) + C_{4,j}\cosh(\zeta_j x), \tag{20}$$

with

$$\zeta_j^4 = \frac{m_j\omega_{n,\infty}^2}{EI_{\infty,j}}. \tag{21}$$

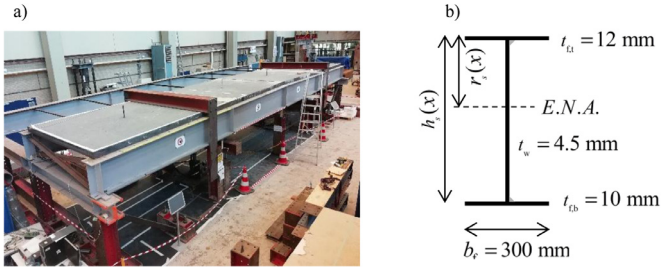

Fig. 3. (a) Overview of the composite beam presented in the work of Nijgh et al. [9]. (b) Cross-sectional dimensions of the tapered steel beam.

The corresponding internal actions are given by

$$M_j = EI_{\infty,j}\frac{d^2\widetilde{w}_j}{dx^2}, \tag{22}$$

$$V_j = \frac{dM_j}{dx}. \tag{23}$$

The 4 • J integration constants, resulting from the J segments in which Eq. (20) is defined, can be solved by imposing boundary conditions at x_0 and x_J, and interface conditions at $x_1 \ldots x_{J-1}$. For a simply supported beam supported at $x_0 = 0$ and $x_J = L$, the boundary conditions at the supports are $w_1(0) = 0$, $w_J(L) = 0$, $M_1(0) = 0$ and $M_J(L) = 0$. The interface conditions are expressed as $\widetilde{w}_j(x_j) = \widetilde{w}_{j+1}(x_j)$, $\widetilde{w}'_j(x_j) = \widetilde{w}'_{j+1}(x_j)$, $M_j(x_j) = M_{j+1}(x_j)$, and $V_j(x_j) = V_{j+1}(x_j)$. It should be noted that the full beam must be modelled to find all eigenfrequencies and –modes: if symmetry conditions are used, only the odd-numbered eigenfrequencies and -modes (n = 1,3,5,…) can be found.

By inserting the boundary conditions into the general solutions, a system of J homogeneous equations is obtained. The system of homogenous equations can be written as

$$[A]\{c\} = \{0\}, \tag{24}$$

in which $\{c\} = [C_{1,1}C_{2,1}\ldots C_{5,J}C_{6,J}]$ and [A] is the coefficient matrix. Non-trivial solutions of Eq. (24) can only be found if the determinant of the coefficient matrix is zero, hence if

$$\det[A] = 0. \tag{25}$$

In case $\det[A] = 0$, the angular eigenfrequency ω_n was assumed correctly in Eq. (21). In case $\det[A] \neq 0$, another trial solution must be adopted to find the angular eigenfrequency. Wu et al. [32] proposed to find the angular eigenfrequency by stepping through a sequence of small increments of ω_n and computing the sign for the determinant of [A]. If the sign of the determinant of [A] changes, an approximation for the angular eigenfrequency is obtained, which can be further refined using the bisection method.

After determining ω_n such that $\det[A] = 0$, the eigenfrequency of the composite beam with rigid shear connection can be determined based on Eq. (18). The eigenfrequency for a composite beam with a flexible shear connection can then be determined using the proposed expression in Eq. (14). The parameters w_m and $w_{m,\infty}$ in Eq. (14) can be determined using the analytical method presented in Section 2.1.

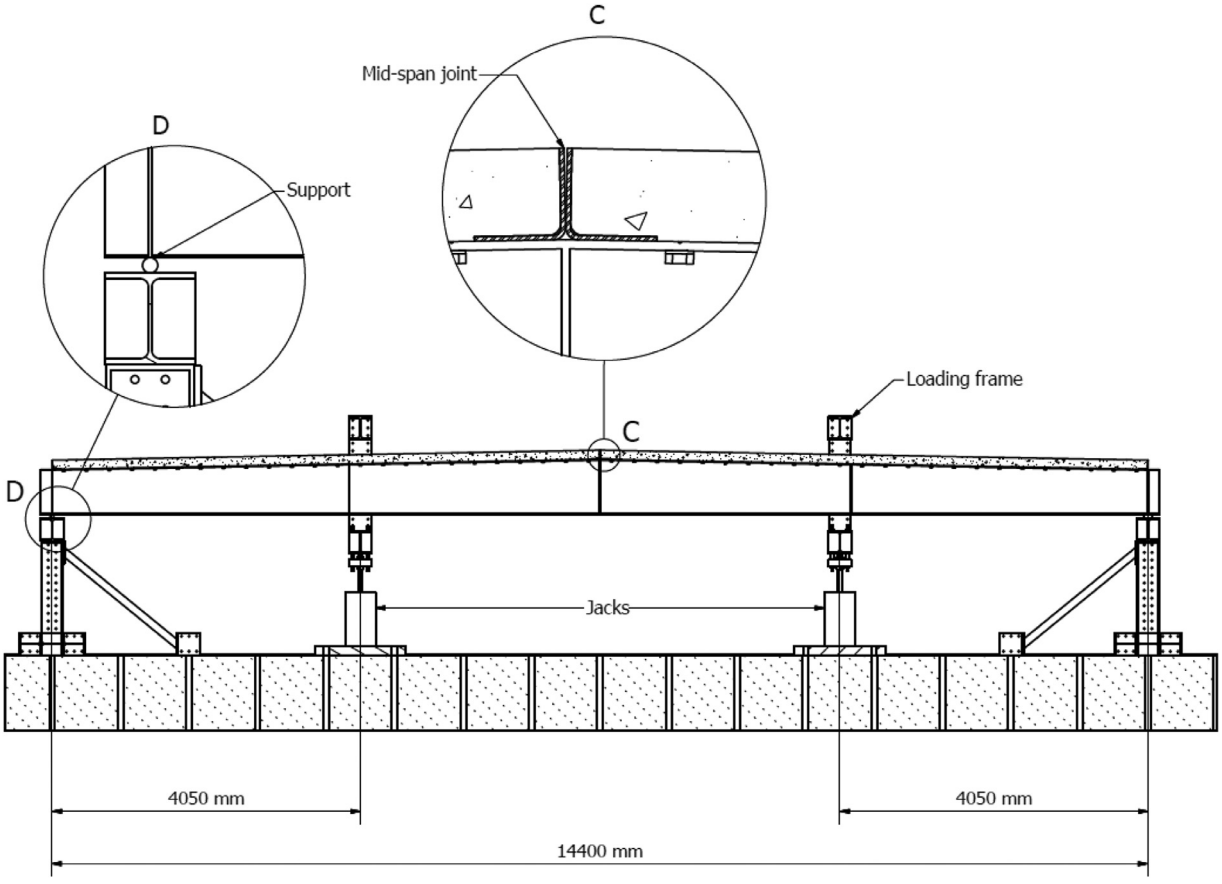

Fig. 4. Cross-section (side-view) of composite beam studied by Nijgh et al. [9]. Two prefabricated solid concrete decks are supported by two tapered steel beams with a span of 14.4 m. Loads are applied at 4.05 m from the supports. The c.t.c. distance between the steel beams is 2.6 m.

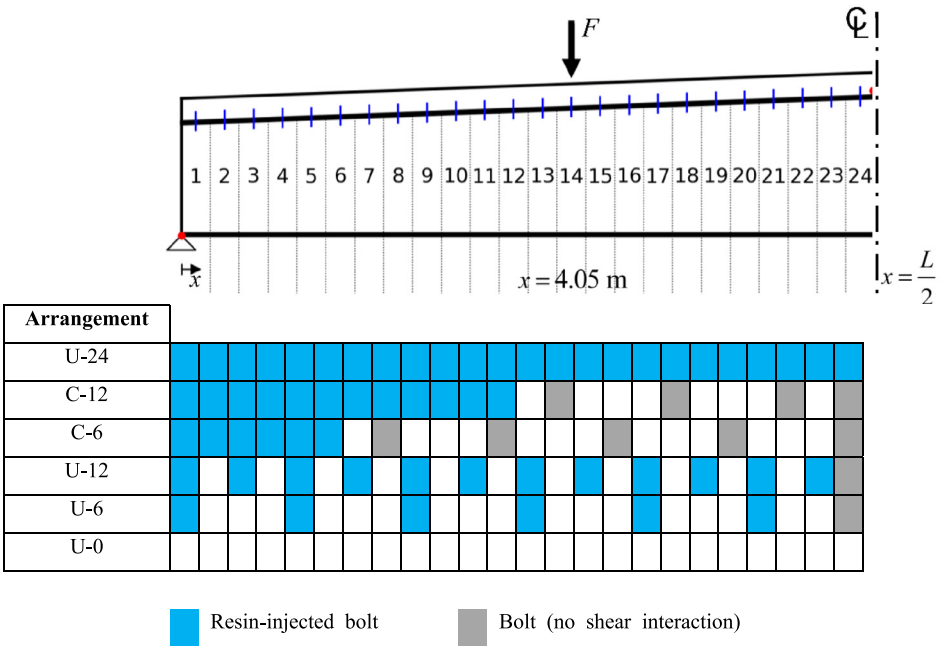

Fig. 5. Shear connector arrangements considered in the work of Nijgh et al. [9]. Each coloured box indicates a pair of fasteners (one per steel beam). Resin-injected bolts provide shear connection; normal bolts are placed only to prevent vertical separation of the deck and beam. "U" denotes uniform connector spacing, "C" denotes concentrated connector spacing near the supports. The beam is symmetric in the plane at $x = L/2$. (For interpretation of the references to colour in this figure legend, the reader is referred to the web version of this article.)

3. Comparison with experimental/numerical results and discussion

3.1. Static analysis

The analytical method presented in Section 2.1 is validated against actual beam tests performed by Nijgh et al. [9] on tapered prefabricated composite beams with various shear connector arrangements. The simply-supported composite beam (see Fig. 3a) consists of two prefabricated solid concrete decks of 7.2 m by 2.6 m, connected to two symmetrically tapered steel beams using demountable shear connectors. The composite beam spans 14.4 m and is subjected to bending by applying point loads at 4.05 m from the supports. A schematic drawing of the specimen is shown in Fig. 4. The height of the symmetrically tapered steel beams varies linearly between the supports, $h_s(x=0;\ x=L)=590$mm, and midspan, $h_s(x=L/2)=725$ mm. The cross-sectional dimensions of the tapered steel beam are presented in Fig. 3b. The concrete deck has a constant thickness of 120 mm along its length and it is assumed that $E_{deck}=33$GPa [33]. The shear connector stiffness k_{sc} was previously determined as 55 kN/mm [9]. The shear connector arrangements presented in Fig. 5 were considered in the experimental programme.

A sensitivity study is carried out to determine the minimum number of beam segments per half-span (J) that are necessary to be modelled, such that the deflection at midspan based on J segments converges to the value obtained for $J\to\infty$. This analysis is performed under the assumption of a uniformly distributed load and a uniformly distributed shear connection with $K=367$kN/mm^2 (equivalent to shear connector arrangement U-24) for the composite beam previously introduced. The results of this sensitivity study are presented in Fig. 6, indicating that a small number of segments is sufficient for convergence of the deflection at midspan. For $J\geq 3$ the error regarding midspan deflection compared with $J\to\infty$ is smaller than 1%. As the experimental beam [9] offers the possibility to install 24 pairs of shear connectors in each half-span, the theoretical beam is conveniently subdivided into $J=24$ segments per half-span.

The results obtained using the proposed analytical method are listed in Table 1, together with the experimental and finite-element results obtained by Nijgh et al. [9]. The results are expressed in terms of the effective bending stiffness and the effective shear stiffness of the composite beam, respectively defined as

$$k_{b,eff}=\frac{\Delta F}{\Delta w(x=L/2)};\ k_{s,eff}=\frac{\Delta F}{\Delta u(x=0)}. \tag{26}$$

In Eq. (26), ΔF is the force increment, $\Delta W(x=L/2)$ is the deflection increment at midspan and $\Delta u(x=0)$ is the slip increment at the supports. These parameters were evaluated at linear-elastic load levels.

Fig. 7, Fig. 8 and Table 1 clearly show that the proposed analytical model and the finite element results [9] are in good agreement regarding the effective bending stiffness and the effective shear stiffness for all the considered shear connector arrangements. The numerical and analytical predictions closely match the experimental results regarding the effective bending stiffness, with average deviations of only 0.4% and 2.4%, respectively. Large deviation exists regarding the effective shear stiffness, as was already observed in [9]. On average, the actual end-slip is 47% smaller than predicted using the proposed analytical model. The source of this deviation is not considered in this paper. The proposed analytical model, however, shows good agreement with the finite element model [9] with an average deviation of only 6%. This indicates that the large deviation between analytical model and experimental results is likely related to the experiments and not to the present analytical model nor to the finite element analysis [9].

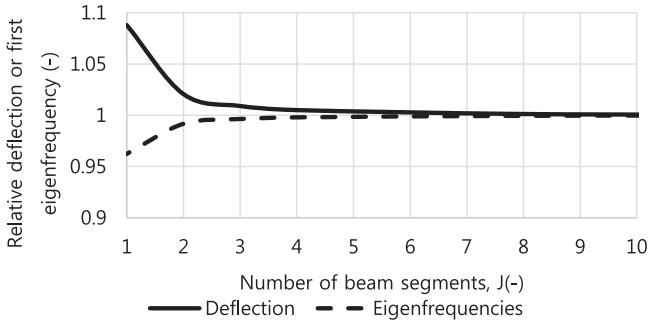

Fig. 6. Relative deflection of the tapered composite beam subject to a uniformly distributed load, as a function of the number of segments J per half-span.

Table 1
Results obtained using proposed analytical model (present study) and the experimentally and numerically obtained results by Nijgh et al. [9] regarding effective bending stiffness and effective shear stiffness for the considered shear connector arrangements.

	$k_{b,eff}$(kN/mm)			$k_{s,eff}$(kN/mm)		
Arrangement	Analytical model	Experiment	FE model	Analytical model	Experiment	FE model
U-24	7.25	6.89	7.13	285	514	301
C-12	7.04	6.69	6.96	269	487	294
C-6	6.31	6.18	6.28	190	389	188
U-12	6.60	6.35	6.53	177	330	190
U-6	5.90	5.82	5.87	120	199	128
U-0	3.96	4.10	4.07	46	98	51

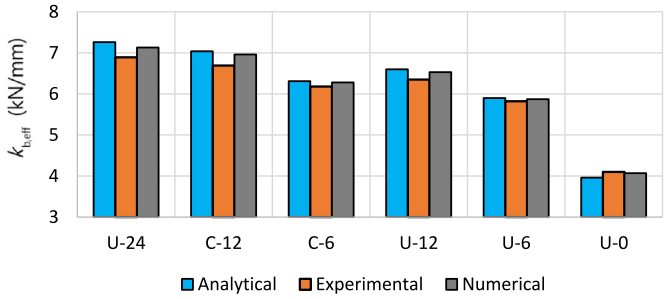

Fig. 7. The effective bending stiffness parameter obtained using the proposed analytical method, compared with the experimentally and numerically obtained results [9], for the different shear connector arrangements.

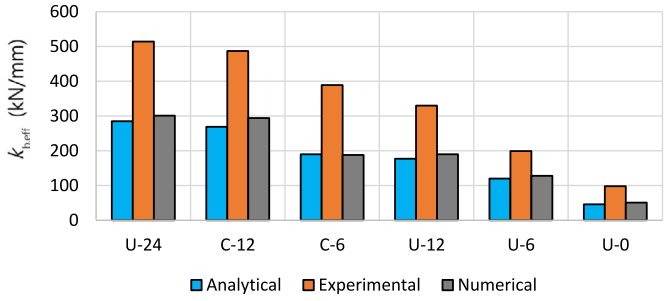

Fig. 8. The effective shear stiffness parameter obtained using the proposed analytical method, compared with the experimentally and numerically obtained results [9], for the different shear connector arrangements.

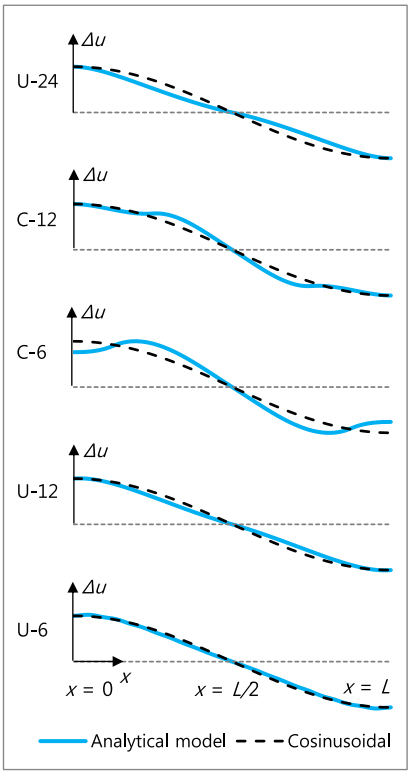

Fig. 9. Shape of slip distribution along the length of the tapered composite beam subjected to a uniformly distributed load q ($F = 0$), compared to the cosinusoidal distribution assumed by Lawson et al. [19].

Present study confirms that the deflection and shear connector slip can be minimized by concentrating the shear connectors near the supports of a simply supported beam. By optimizing the shear connector arrangement the total number of shear connectors can be reduced, which has a positive impact on the speed of (de)construction and the material and labour costs. Both parameters are key to the successful implementation of demountable and reusable structures within the construction industry [8].

The slip distribution along the tapered composite beam subjected to a uniformly distributed load q ($F = 0$) is shown in Fig. 9 for the different shear connector arrangements. This load case corresponds to a practical beam application. Fig. 9 indicates that the assumption of Lawson et al. [19] of a cosinusoidal shape function for the interlayer slip is not generically valid: particularly in the case of shear connectors concentrated near the supports (arrangements C6 and C12) a more refined analysis using the present method must be carried out to determine the actual slip distribution and the corresponding internal actions.

3.2. Free vibration analysis

The first eigenfrequency of the tapered composite beam presented in Section 3.1 is determined for the shear connector arrangements listed in Fig. 5 and for various magnitudes of the shear connector stiffness k_{sc} (25, 55 and 100 kN/mm). In this analysis, the composite beam is regarded as part of a larger structure and that therefore one tapered composite beam effectively consists of one tapered steel beam and two prefabricated concrete decks.

The results of a sensitivity study to determine the minimum number of beam segments per half-span J to ensure an accurately prediction of the first eigenfrequency are presented in Fig. 6. The analysis has been conducted with the same assumptions as for the sensitivity study regarding the deflection. Also in this case it is found that for $J \geq 3$ the convergence error in terms of first eigenfrequency is smaller than 1%. All calculations are carried out by subdividing the beam into $J = 24$ segments per half-span to match the segmentation used in Section 3.1.

The analytical method to determine the eigenfrequencies of a non-prismatic composite beam with flexible shear connectors is validated by

Table 2
First eigenfrequencies of the tapered composite beam presented in Section 3.1 for various shear connector arrangements and shear connector stiffness, obtained using the proposed analytical model and using finite element analysis.

Arrangement	$f_{n,\infty,\text{FEA}}$ (Hz)	$f_{n,\infty,\text{analytical}}$ (Hz)	k_{sc} (kN/mm)	$w_{m,\infty}/w_m$ (-)	$f_{n,\text{analytical}}$ (Hz)	$f_{n,\text{FEA}}$ (Hz)	$f_{n,\text{analytical}}/f_{n,\text{FEA}}$ (-)
U-24	5.39	5.51	25	0.82	4.99	5.00	0.998
			55	0.9	5.23	5.17	1.012
			100	0.94	5.34	5.25	1.017
C-12			25	0.79	4.88	4.92	0.992
			55	0.87	5.14	5.10	1.007
			100	0.92	5.27	5.20	1.013
C-6			25	0.69	4.59	4.71	0.975
			55	0.78	4.88	4.89	0.997
			100	0.84	5.03	5.00	1.007
U-12			25	0.73	4.71	4.81	0.978
			55	0.84	5.04	5.02	1.002
			100	0.9	5.22	5.15	1.013
U-6			25	0.64	4.41	4.61	0.957
			55	0.75	4.78	4.85	0.987
			100	0.83	5.02	5.00	1.004
U-0			0	0.44	3.65	3.67	0.995
Average							0.997

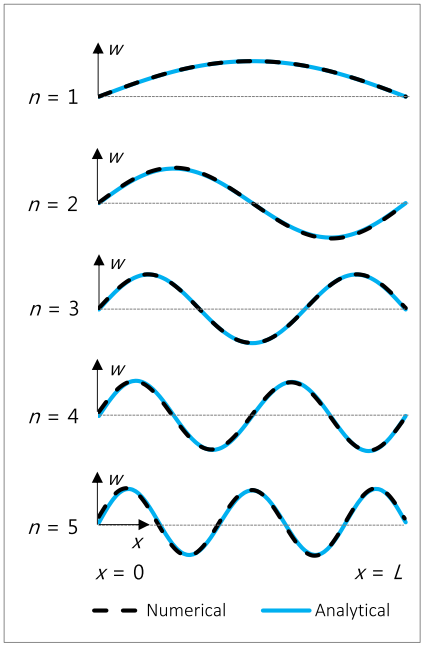

Fig. 10. Eigenmodes of the tapered composite beam.

finite element analysis. The simply supported composite beam is modelled in ABAQUS/Standard using four-node shell elements (S4) for the tapered steel beam and concrete deck. The shear connectors are modelled using mesh-independent, point-based fasteners with a spring stiffness equal to k_{sc}.

The results obtained using the analytical and numerical models are presented in Table 2. On average, the first eigenfrequency obtained by the proposed analytical model is 0.3% lower than predicted by the finite element model. The first eigenfrequency is underestimated in case of a weak shear connection and overestimated in case of a strong shear connection, with a maximum deviation of 4.3% for the U-6 case with $k_{sc} = 25$ kN/mm. The proposed analytical model is therefore considered suitable for determination of the first eigenfrequency of a tapered composite beam with non-uniform shear connector arrangements.

Fig. 10 shows the first five natural vibration modes of the tapered composite beam. Good agreement between the analytical model and finite element model is observed in terms of modal shape. The higher order natural frequencies of the tapered composite beam are listed in Table 3. It is observed that the higher-order natural frequencies are not equal to $f_1 n^2$, as is the case for prismatic beams, but are slightly smaller because of the non-uniform mass and bending stiffness distributions.

Table 3
Natural frequencies for the tapered composite beam with a rigid shear connection.

n (-)	$f_{n,\infty,\text{analytical}}$ (Hz)	$\sqrt{\frac{f_{1,\infty,\text{analytical}}}{f_{n,\infty,\text{analytical}}}}$ (-)
1	5.51	1.00
2	21.2	1.96
3	47.9	2.94
4	84.7	3.92
5	132.5	4.90

5. Conclusions

The main outcomes of the theoretical and numerical assessment of the deflection and first eigenfrequencies of (reusable) tapered composite beams are as follows:

- The proposed analytical methods provide an easy to use formulation to assess the structural response of a composite beam in the elastic stage.
- The proposed analytical method requires discretisation into a limited number of segments along the beam length to obtain accurate results. Discretising the beam into 3 segments per half-span leads to convergence of the deflection and the first eigenfrequency for the composite beam studied in this work.
- The proposed analytical method accurately predicts the deflection of tapered composite beams. On average, the deviation of the proposed analytical method regarding midspan deflection is 2.4 % compared with the experimental results and 0.4% compared with the finite element results of Nijgh et al. [9].
- Predictions regarding end slip obtained using the proposed analytical method are in line with finite element analysis, with an average deviation of 6%. The analytical and numerical model do not reproduce the end slip obtained in the experimental work of Nijgh et al. [9]. Discussion of reasons for such scattering is left out of the scope of this work.

- The shape of the slip distribution along the length of a non-prismatic composite beam is not necessarily cosinusoidal, particularly for non-uniform shear connector arrangements. This limits the validity of the Lawson model [19]. Therefore, it is recommended to use present method to determine the actual slip distribution and the corresponding internal actions.
- Very good agreement is found between the eigenfrequencies obtained using finite element analysis and the proposed analytical model. On average, the proposed analytical model underestimates the first eigenfrequency by 0.3%.

Acknowledgment

This research was carried out under project number T16045 in the framework of the Research Program of the Materials innovation institute M2i (www.m2i.nl) supported by the Dutch government.

References

[1] Shaikh AF, Yi W. In-place strength of welded headed studs. PCI J 1985;30(2):56–81.
[2] Mirza O, Uy B. Effects of the combination of axial and shear loading on the behaviour of headed stud steel anchors. Eng Struct 2010;32(1):93–105.
[3] Lam D, El-Lobody E. Behavior of headed stud shear connectors in composite beam. J Struct Eng 2005;131(1):96–107.
[4] Hanswille G, Porsch M, Ustundag C. Resistance of headed studs subjected to fatigue loading: Part I: experimental study. J Construct Steel Res 2007;63(4):475–84.
[5] Pavlovic M. Resistance of bolted shear connectors in prefabricated steel-concrete composite decks. Belgrade: University of Belgrade; 2013.
[6] Moynihan MC, Allwood JM. Viability and performance of demountable composite connectors. J Construct Steel Res 2014;99:47–56.
[7] van den Dobbelsteen A. The sustainable office - an exploration of the potential for factor 20 environmental improvement of office accommodation. Delft: Delft University of Technology; 2004.
[8] Tingly DD, Davinson B. Design for deconstruction and material reuse. In: Proceedings of the institution of civil engineers, 164; 2011. p. 195–204.
[9] Nijgh MP, Girbacea IA, Veljkovic M. Elastic behaviour of a reusable tapered composite beam. Eng Struct 2019;183.
[10] Roberts TM. Finite difference analysis of composite beams with partial interaction. Comput Struct 1985;21(3):469–73.
[11] Lin JP, Wang G, Bao G, Xu R. Stiffness matrix for the analysis and design of partial-interaction composite beams. Construct Build Mater 2017;156:761–72.
[12] Ranzi G, Gara F, Leoni G, Bradford MA. Analysis of composite beams with partial shear interaction using available modelling techniques: a comparative study. Comput Struct 2006;84:930–41.
[13] Newmark NM, Siest CP, Viest CP. Test and analysis of composite beams with incomplete interaction. In: Proceedings of the Society for Experimental Stress Analysis; 1951. p. 75–92.
[14] Girhammar UA, Pan DH. Exact static analysis of partially composite beams and beam-columns. Int J Mech Sci 2007;49:239–55.
[15] Girhammar UA. A simplified analysis method for composite beams with interlayer slip. Int J Mech Sci 2009;51:515–30.
[16] Xu R, Wu Y. Static, dynamic, and buckling analysis of partial interaction composite members using Timoshenko's beam theory. Int J Mech Sci 2007;49:1139–55.
[17] Schnabl S, Saje M, Turk G, Planinc I. Analytical solution of two-layer beam taking into account interlayer slip and shear deformation. J Struct Eng 2007;133(6):886–94.
[18] Yam LCP, Chapman JC. The inelastic behaviour of simply supported composite beams of steel and concrete. In: Proceedings of the institution of civil engineers, 41; 1968. p. 651–83.
[19] Lawson RM, Lam D, Aggelopoulos ES, Nellinger S. Serviceability performance of composite beams. In: Proceedings of the institution of civil engineers, 170; 2017. p. 98–114.
[20] Adekola AO. Partial interaction between elastically connected elements of a composite beam. Int J Solids Struct 1968;4:1125–35.
[21] Al-Amery RIM, Roberts TM. Non-linear finite difference analysis of composite beams with partial interaction. Comput Struct 1990;35(1):81–7.
[22] Hirst MJS, Yeo MF. The analysis of composite beams using standard finite element programs. Comput Struct 1980;11:233–7.
[23] Salari MR, Spacone E, Shing PB, Frangopol DM. Nonlinear analysis of composite beams with deformable shear connectors. J Struct Eng 1998;124(10):1148–58.
[24] Zona A, Ranzi G. Finite element models for nonlinear analysis of steel-concrete composite beams with partial interaction in combined bending and shear. Finite Elem Anal Des 2011;47:98–118.
[25] Schnabl S, Saje M, Turk G, Planinc I. Locking-free two-layer Timoshenko beam element with interlayer slip. Finite Elem Anal Des 2007;43:705–14.
[26] Chakrabarti A, Sheikh AH, Griffith M, Oehlers DJ. Analysis of composite beams with partial shear interaction using a higher order beam theory. Eng Struct 2012;36:283–91.
[27] Uddin MA, Sheikh AH, Brown D, Bennet T, Uy B. A higher order model for inelastic response of composite beams with interfacial slip using a dissipation based arc-length method. Eng Struct 2017;139:120–34.
[28] Ranzi G, Bradford MA, Uy B. A direct stiffness analysis of a composite beam with partial interaction. Int J Numerical Methods Eng 2004;61:657–72.
[29] Ranzi G, Bradford MA. Analysis of composite beams with partial interaction using the direct stiffness approach accounting for time effects. Int J Numerical Methods Eng 2009;78:564–86.
[30] Girhammar UA, Pan DH, Gustafsson A. Exact dynamic analysis of composit beams with partial interaction. Int J Mech Sci 2009;51:565–82.
[31] Taleb NJ, Suppiger EW. Vibration of stepped beams. J Aerosp Eng 1961;28:295–8.
[32] Wu YF, Xu R, Chen W. Free vibrations of the partial-interaction composite members with axial force. J Sounds Vibrations 2007;299:1074–93.
[33] NEN. EN 1992-1-1: Eurocode 2: design of concrete structures - Part 1-1: general rules and rules for buildings. Delft: NEN; 2005.